

# INTERNATIONAL SOCIETY FOR SOIL MECHANICS AND GEOTECHNICAL ENGINEERING



*This paper was downloaded from the Online Library of the International Society for Soil Mechanics and Geotechnical Engineering (ISSMGE). The library is available here:*

<https://www.issmge.org/publications/online-library>

*This is an open-access database that archives thousands of papers published under the Auspices of the ISSMGE and maintained by the Innovation and Development Committee of ISSMGE.*

*The paper was published in the proceedings of the 7<sup>th</sup> International Conference on Earthquake Geotechnical Engineering and was edited by Francesco Silvestri, Nicola Moraci and Susanna Antonielli. The conference was held in Rome, Italy, 17 - 20 June 2019.*

# A multi-directional numerical approach for the seismic ground response and dynamic soil-structure interaction analyses

A. di Lernia

*Department of Civil, Environmental, Building Engineering and Chemistry, Politecnico di Bari, Italy*

A. Amorosi

*Department of Structural and Geotechnical Engineering, Sapienza University of Rome, Italy*

D. Boldini

*Department of Civil, Chemical, Environmental and Materials Engineering, University of Bologna, Italy*

**ABSTRACT:** This paper describes a numerical approach for the analysis of the seismic ground response and the dynamic soil-structure interaction accounting for the three components of an earthquake motion. The investigation was performed with reference to the case-history of Lotung (Taiwan), where the seismic response of a nuclear power plant model as well as that of its foundation soil were measured during several earthquakes occurred at the site. The numerical analyses were carried out with the finite element code Plaxis, adopting for the soil the constitutive model Hardening Soil model with small strain stiffness. First, the model was validated with respect to the propagation of the vertical component of seismic motion, mainly associated to compressional seismic waves. Then fully 3D dynamic analyses were implemented for the simulation of the strong motion event named LSST7. The good match between numerical predictions and monitoring data proved the effectiveness of the proposed approach.

## 1 INTRODUCTION

The seismic site response analyses are traditionally performed under one-dimensional wave propagation conditions, usually considering only one horizontal component of the seismic motion. Nevertheless, due to the increasing observations of strong vertical ground motion during recent earthquakes, an accurate reproduction of the wave propagation processes should account for the coexistence of all the three components of the seismic motion, i.e. the two horizontal and the vertical ones (e.g. Han et al. 2017). In fact, the three-dimensional nature of the problem may affect the response of the ground and that of any structure located at the surface. This issue is worth being investigated numerically, aiming at highlighting its fundamental nature and its potential consequences in the solution of earthquake-related civil engineering problems.

Recently, a number of research papers have focused the attention on the characteristics of the compressional wave propagation mechanism, mainly associated to the vertical component of the ground motion, as well as on its numerical simulation in the context of finite element analyses (e.g. Han et al. 2016a, Tsaparli et al. 2017). The influence of this wave component can be particularly significant for the seismic design of strategic structures, such as nuclear power plants and large dams (Han et al. 2016b), and for the correct prediction of liquefaction phenomena (e.g. Tsaparli et al. 2016).

A 3D finite element model is here employed to perform multi-directional non-linear site response and dynamic soil-structure interaction (SSI) analyses. The adopted constitutive model for simulating the soil behaviour is the isotropic hardening elasto-plastic hysteretic “Hardening Soil Model with Small-Strain Stiffness” (*HS<sub>small</sub>*) model, capable of describing stress dependency of the stiffness moduli, hysteretic soil non-linearity and plastic-induced accumulation of permanent displacements.

The reliability of the proposed FE approach is assessed by comparing the numerical predictions with the recorded motions obtained from the Lotung LSST site. The experimental LSST site was extensively instrumented to record both the ground response, through surface and downhole arrays, and the structural response of a small-scale nuclear power plant containment structure.

The proposed numerical approach was already validated for the bi-directional wave propagation problem by simultaneously applying the horizontal components of the recorded seismic motion, disregarding the effect of the vertical component of earthquakes (Amorosi et al. 2016, Amorosi et al. 2017). Herein, the three components of a strong-motion earthquake that shook the site in 1986, named LSST7, are considered as input motions. The three-dimensional response of the model is investigated by simultaneously applying the two horizontal components of the acceleration time histories together with the vertical one. The results demonstrate that the numerical back-predictions are in fair agreement with the monitored data along all the three directions of the considered seismic motions.

## 2 LOTUNG CASE STUDY

The Large-Scale Seismic Test (LSST) was a research programme established in 1985 at Lotung, a highly seismic region in the North-East of Taiwan, for the purpose of studying the effects of soil-structure interaction on the dynamic response of nuclear power plant containment structures (EPRI, 1991). More specifically, a 1/4 scaled-down model of a nuclear power plant containment structure was built at the site. It consisted in a reinforced concrete cylindrical shell structure of external radius of 10.52 m and constant thickness of 0.305 m, for a total height of 15.24 m, of which 4.57 m embedded into the soil below the ground surface. The model was extensively instrumented, together with its foundation soil, to record both the structural and ground seismic responses during earthquakes (Figure 1). SSI effects were found to have a considerable influence on the seismic response of the monitored structures, due to their very high stiffness and mass and to the local relatively soft soil conditions (Amorosi et al. 2015a, Amorosi et al. 2015b, Amorosi et al. 2017).

The local soil profile at the LSST site is characterised by a layer of silty sand extending from the surface down to a depth of 17 m, overlying a 6 m thick layer of sand with gravel. Underneath the sand layers, a stratum of silty clay extends to the maximum investigated depth of 47 m and is interlayered by an inclusion of sand with gravel between 29 m and 36 m of depth (Figure 2). The few available information on the ground water level indicate for it a depth of 1 m below the ground surface. The geotechnical characterisation of the soil deposit is based on the available in-situ tests and the back-analyses of seismic data found in the literature and synthesized in Amorosi et al. (2016). The profiles of shear and longitudinal wave velocities, shown in Figure 2, were obtained by geophysical tests executed in the area down to 47 m. The distribution of  $V_s$  with depth points out the soft nature of the soil deposit, as it varies from about 100 m/s at the ground surface to 300 m/s at 47 m depth.

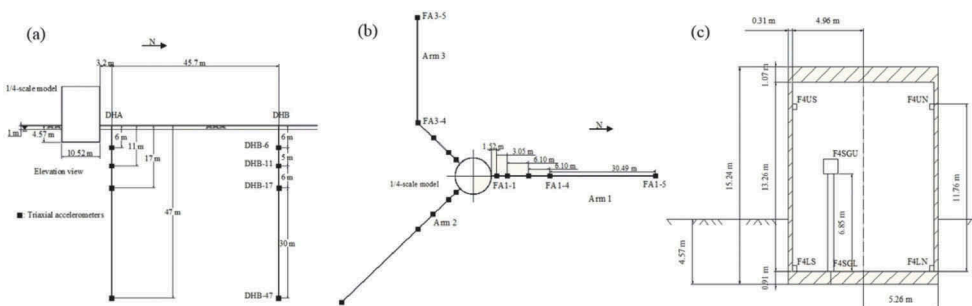


Figure 1. Location of surface, downhole and structural instrumentation at Lotung LSST site: (a) down-hole arrays, (b) surface arrays and (c) accelerometers on the 1/4-scale containment model (modified from Amorosi et al. 2016 and Amorosi et al. 2017)

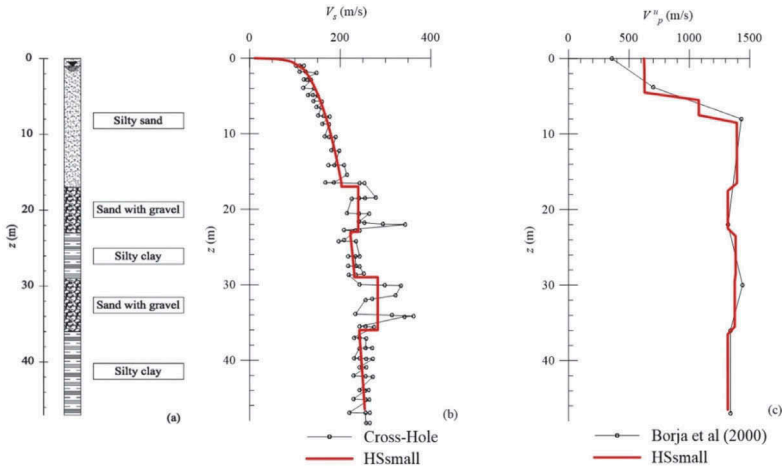


Figure 2. Local soil profile at Lotung LSST site: (a) soil stratigraphy, (b) S-wave velocity and (c) P-wave velocity profiles (modified from Amorosi et al. 2016 and Amorosi et al. 2017)

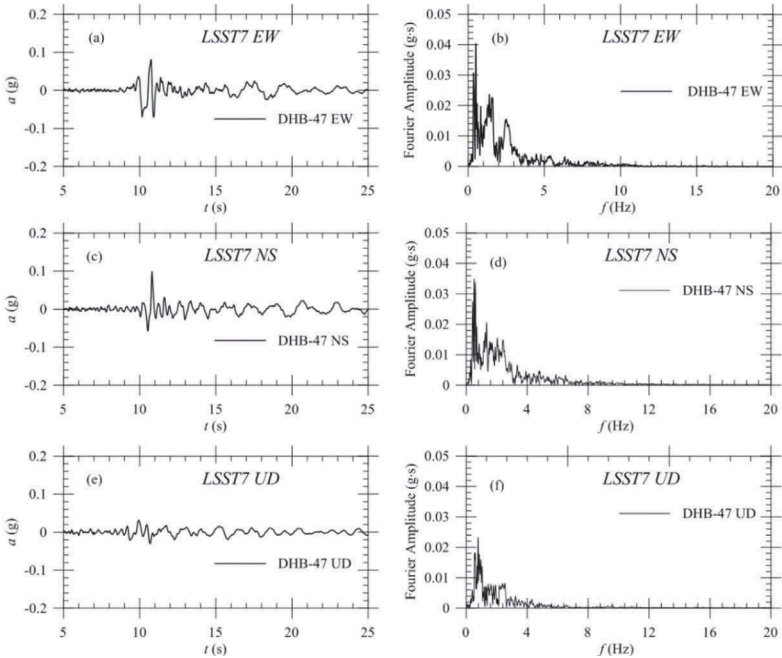


Figure 3. Acceleration time histories and corresponding Fourier spectra of the (a, b) EW, (c, d) NS and (e, f) UD components of the LSST7 seismic event recorded at DHB-47 (partially modified from Amorosi et al. 2016 and Amorosi et al. 2017)

The non-linear FE numerical investigations were conducted with reference to the strong-motion seismic event LSST7, occurred on May 20th 1986. The acceleration time histories along the three EW, NS and UD directions, recorded at the largest depth by the accelerometer DHB-47 (Figure 1) and shown in Figure 3 together with the corresponding Fourier spectra, are assumed as rigid bedrock motions in the numerical analyses. The seismic signals were preliminary baseline corrected and filtered by a low-pass filter in order to cut off frequencies higher than 20 Hz.

### 3 THE NUMERICAL APPROACH

The numerical analyses were performed with the Finite Element (FE) code PLAXIS (Brinkgreve et al. 2013), assuming undrained conditions during the dynamic stages of the calculation. This hypothesis was considered as sufficiently accurate for the simulation of both S- and P-wave propagation, due to the permeability of the soil strata (Han et al., 2016).

Soil response was modelled with the *HSsmall* constitutive model, available in the library of the code and already successfully adopted by the Authors of this paper in similar geotechnical problems (e.g. Amorosi et al. 2014, Falcone et al. 2018). A summary of the *HSsmall* model parameters adopted for the different soil layers is given in Table 1. They were derived according to the calibration strategy described in Amorosi et al. (2016). More specifically, reference initial shear stiffness modulus  $G_0^{ref}$  and the parameter  $m$  were obtained by best fitting the S-wave velocity profile, as shown in Figure 2. The parameter  $\gamma_{0.7}$  was selected in order to obtain the best approximation of the secant shear modulus and damping ratio decay curves. The elastic unloading-reloading Young's modulus  $E_{ur}^{ref}$  was evaluated such that the ratio  $G_0^{ref}/G_{ur}^{ref}$  results equal to 4 for the silty sand layer and to 2.5 for the other soil layers. Finally, the stiffness parameters  $E_{oed}^{ref}$  and  $E_{50}^{ref}$  were both assumed to be three times lower than  $E_{ur}^{ref}$ .

In the performed analyses, simulations also included the propagation of the vertical component of the ground motion. As such, special care was dedicated to the correct approximation of the P-wave velocity profile (Figure 2), controlled by the following constitutive equations if undrained conditions are assumed:

$$E_{oed,u}^{ref} = E_{oed}^{ref} + \frac{K_w}{n} \quad (1)$$

$$V_p^u = \sqrt{\frac{E_{oed,u}^{ref}}{\rho}} \quad (2)$$

where  $K_w$  is the pore water bulk modulus, assumed equal to  $2.2 \cdot 10^6$  kPa, and  $n$  is the soil porosity, here specifically manipulated to obtain the desired value of the compressional wave velocity  $V_p^u$  under undrained conditions.

FE models (2D and 3D) were characterised by a height equal to that of the investigated soil deposit, e.g. 47 m (Figure 4). A hydrostatic pore pressure distribution from the depth of 1 m b.g.l. was assumed. The FE discretisation was set to ensure the elements' size to be smaller than one-eighth of the wavelength associated with the maximum frequency component of the input signals.

The boundary conditions adopted in the dynamic stages consisted in viscous boundaries at the lateral sides and in the direct application of the input motion components at the base of the model (Figure 4). The standard Newmark method was employed as time integration scheme with parameters  $\beta_1 = 0.6$  and  $\beta_2 = 0.605$  and a time step of 0.005 s.

Table 1. Material parameters

z (m)	n (-)	c (kPa)	$\phi$ (°)	$K_0^{NC}$ (-)	OCR (-)	$v_{ur}$ (-)	$G_0^{ref}$ (MPa)	$E_{ur}^{ref}$ (MPa)	$E_{50}^{ref}$ (MPa)	$E_{oed}^{ref}$ (MPa)	m (-)	$\gamma_{0.7}$ (%)
0–17	0.84	0.01	30	0.50	10	0.30	90	60	20	20	0.54	0.011
0–17	0.65	0.01	30	0.50	10	0.30	90	60	20	20	0.54	0.011
0–17	0.57	0.01	30	0.50	10	0.30	90	60	20	20	0.54	0.011
17–23	0.64	0.01	35	0.43	10	0.29	115	119.5	39.8	39.8	0	0.010
23–29	0.58	10	24	0.59	5	0.25	65	650	21.7	21.7	0.42	0.025
29–36	0.59	0.01	37	0.40	10	0.28	160	164.5	54.8	54.8	0	0.010
36–47	0.64	10	24	0.59	5	0.25	65	65	21.7	21.7	0.42	0.025

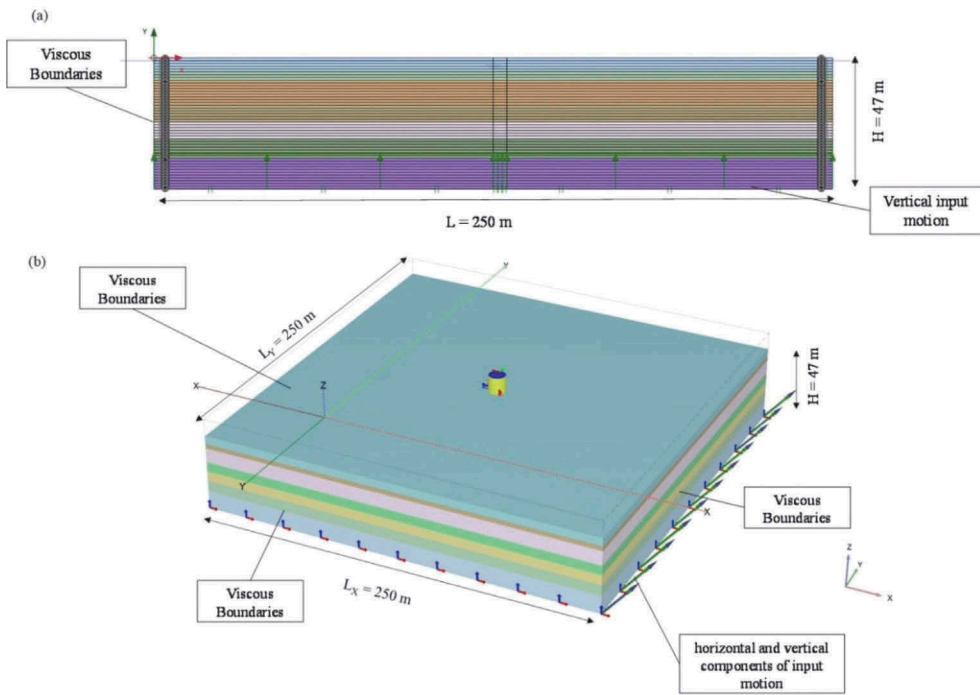


Figure 4. Numerical models employed in the simulations: (a) 2D model adopted in the validation phase of the P-wave propagation process; (b) 3D model used for the dynamic SSI analysis

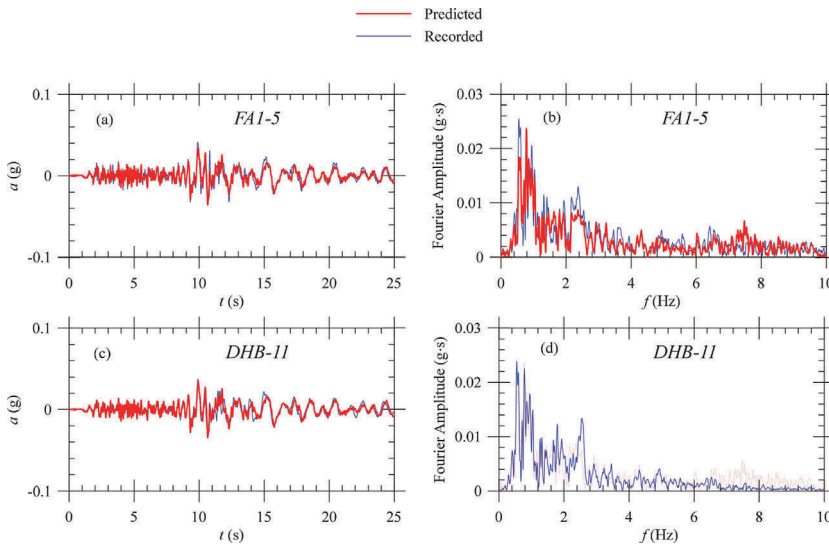


Figure 5. Comparison between recorded and predicted UD vertical response at different depths in terms of acceleration time history and Fourier spectrum: (a, b) 0 m and (c, d) -11 m below ground surface

#### 4 ONE-DIMENSIONAL VERTICAL P-WAVE PROPAGATION

The numerical approach was first validated with reference to the propagation of vertical compressional waves. A 2D finite element model was set up as shown in Figure 4(a), assuming

free-field conditions. The geometrical model adopted for the free field response analysis consisted of a 250 m wide mesh, according to the suggestions proposed by Amorosi et al. (2010).

Figure 5 summarises the comparison between the numerical predictions and monitoring data as observed at depth of 11 m below the ground surface along the downhole array DHB (DHB-11) and at the ground surface at location FA1-5 (Figure 1). A satisfactory agreement can be observed in terms of both acceleration time histories and Fourier spectra, thus indicating a correct simulation of the intensity and frequency content of the analysed ground motion component.

## 5 MULTI-DIRECTIONAL SITE RESPONSE ANALYSIS

In order to investigate the seismic site response under multi-directional free-field conditions, a 3D FE model was employed by applying all the three components of the selected earthquake. The 3D geometrical model was characterised by an extension of 250 m along both horizontal directions, while the vertical thickness is assumed equal to 47 m.

The numerical response is illustrated in terms of acceleration time histories, obtained at ground surface (FA1-5) and at a depth of 11 m (DHB-11) for each direction of motion, and compared against the recorded ones at the same depths (Figure 6). Because of the significant numerical noise generated at high frequency level due to the less dissipative response of the adopted constitutive model under multi-directional excitation (Amorosi et al. 2016), the output signals were filtered by a low-pass filter to a cut-off frequency of 8 Hz.

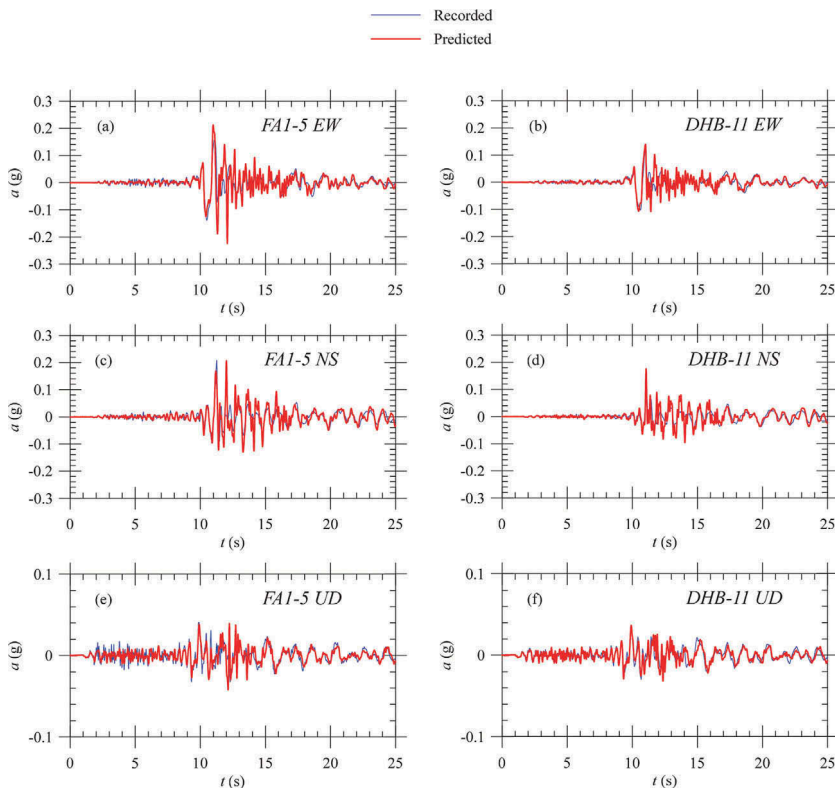


Figure 6. Comparison between recorded and predicted multi-directional free-field response at ground surface (FA1-5) and at depth of 11 m b.g.l. (DHB-11) in terms of acceleration time history: (a, b) EW, (c, d) NS and (e, f) UD components of motion

The comparison shows that the overall response is well captured by the numerical simulation in terms of zero crossings, while a slight over-prediction of the peaks of accelerations is observed for each component at different depth, to be related to the above-mentioned constitutive response of the adopted model.

## 6 MULTI-DIRECTIONAL DYNAMIC RESPONSE OF STRUCTURE

The dynamic response of the containment structure is performed employing the mesh shown in Figure 4b, in which the structure is included. This latter is modelled as a cylindrical plate bounded by two flat circular plates at the roof and the bottom, characterised by linear visco-elastic constitutive response. Typical values of reinforced concrete materials were assumed, i.e. Young's modulus  $E$  equal to  $2.53 \cdot 10^4$  MPa, Poisson's ratio equal to 0.2 and damping ratio equal to 2.5%. This latter is introduced in the FE model by means of the simplified Rayleigh formulation ( $[C]=\beta_R[K]$ ), assuming a control frequency of 10 Hz, a value similar to the fixed-base fundamental frequency of the structure.

The numerical dynamic response of the containment structure is compared to the in-situ recordings at the roof (F4UW and F4US) in terms of acceleration time histories obtained along each component of motion (Figure 7). It can be observed that the dynamic motion predicted at the top of the structural model is in good agreement with that recorded at F4UW along EW and UD directions, as well as at F4US along NS and UD directions. In particular, the peak acceleration of all predicted acceleration time histories matches fairly well the recorded ones.

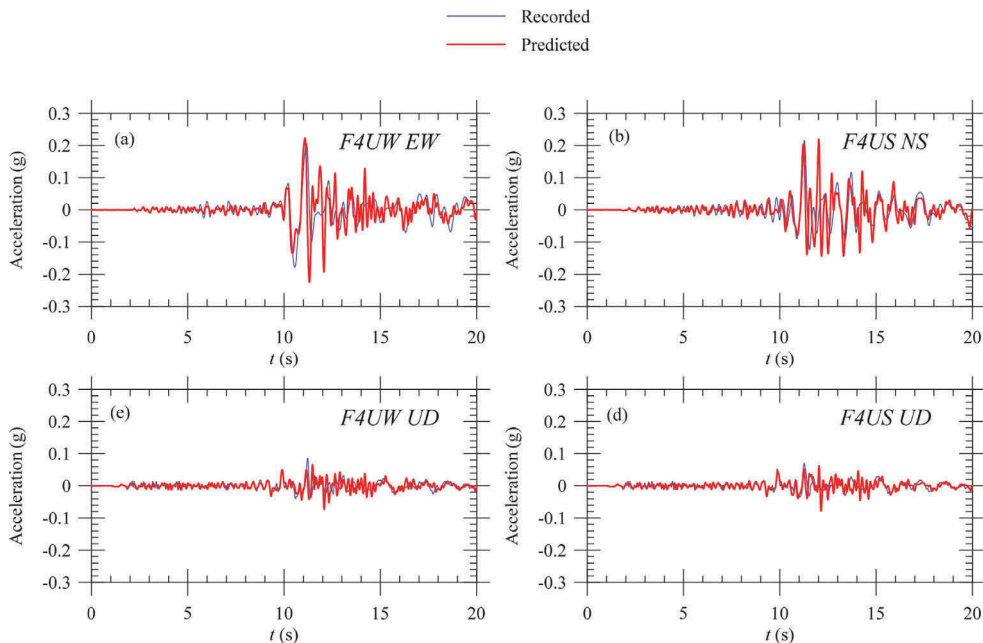


Figure 7. Comparison between recorded and predicted dynamic response of the containment structure at the roof nodes (F4UW, F4US): (a, b) along horizontal directions (EW, NS) and (c, d) along vertical direction (UD)

## 7 CONCLUSIONS

The paper presents a FE numerical approach for the analysis of the seismic ground response and the dynamic soil-structure interaction under multi-directional earthquake motion, with reference to the case study of Lotung LSST. The nonlinear soil behaviour was described by the isotropic hardening elasto-plastic model *HSsmall*, opportunely calibrated in order to catch both the shear and compressional cyclic soil response.

The numerical approach was firstly validated in order to assess the capability of the model of reproducing the vertical site response. The 2D numerical results proved to be in good agreement with the free-field recorded motions. Furthermore, the fully 3D numerical approach was adopted to back-analyse the dynamic behaviour of the nuclear power plant containment structure under both horizontal and vertical site motion. The fairly good matching of numerical acceleration time histories with the recorded ones confirmed the reliability of the adopted FE approach in simulating the multi-directional P- and S- waves propagation processes, providing the accurate calibration of material parameters governing both shear and compressional response.

## REFERENCES

- Amorosi, A., Boldini, D., Falcone, G. 2014. Numerical prediction of tunnel performance during centrifuge dynamic tests. *Acta Geotechnica*. 9(4): 581–596.
- Amorosi, A., Boldini, D., di Lernia, A., Rollo, F. 2015a. Three-dimensional advanced numerical approaches to the seismic soil and structural response analyses. In Giorgio Monti and Gianfranco Valente (eds.), *4th International Workshop on Dynamic Interaction of Soil and Structure, Rome, 12–13 November 2015*. L'Aquila: DISS\_Edition.
- Amorosi, A., Boldini, D., di Lernia, A., 2015b. Advanced numerical approaches to the seismic soil and structural response analyses. In SECED 2015 (ed.), *Earthquake Risk and Engineering towards a Resilient World, Cambridge, 9–10 July 2015*.
- Amorosi, A., Boldini, D., di Lernia, A. 2016. Seismic ground response at Lotung: Hysteretic elasto-plastic-based 3D analyses. *Soil Dynamics and Earthquake Engineering* 85: 44–61.
- Amorosi, A., Boldini, D., di Lernia, A. 2017. Dynamic soil-structure interaction: A three-dimensional numerical approach and its application to the Lotung case study. *Computers and Geotechnics* 90: 34–54.
- Brinkgreve, R.B.J., Engin, E., Swolfs, W.M., 2013. Plaxis 3D. Reference manual.
- EPRI 1991. *Post-Earthquake analysis and data correlation for the 1/4-scale containment model of the Lotung Experiment*. Report No NP-7305-SL. Palo Alto, California.
- Han, B., Zdravkovic, L. & Kontoe, S., 2016a. Numerical and analytical investigation of compressional wave propagation in saturated soils. *Computers and Geotechnics* 75: 93–102.
- Han, B., Zdravkovic, L., Kontoe, S., Taborda, D.M.G. 2016b. Numerical investigation of the response of the Yele rockfill dam during the 2008 Wenchuan earthquake. *Soil dynamics and Earthquake Engineering* 88: 124–142.
- Han, B., Zdravkovic, L., Kontoe, S., Taborda, D.M.G. 2017. Numerical investigation of multi-directional site response based on KiK-net downhole array monitoring data. *Computers and Geotechnics* 89: 55–70.
- Falcone, G., Boldini, D., Amorosi, A. 2018. Site response analysis of an urban area: a multi-dimensional and non-linear approach. *Soil Dynamics and Earthquake Engineering* 109: 33–45.
- Tsaparli, V., Kontoe, S., Taborda, D.M.G., Potts, D.M. 2016. Vertical ground motion and its effects on liquefaction resistance of fully saturated sand deposits. *Proc. R. Soc. A Math. Phys. Eng. Sci.* 472: 21 pages.
- Tsaparli, V., Kontoe, S., Taborda, D.M.G., Potts, D.M. 2017. The importance of accurate time-integration in the numerical modelling of P-wave propagation. *Computers and Geotechnics* 86: 203–208.